Louisiana State University
LSU Digital Commons

Faculty Publications | Department of Physics & Astronomy

2-1-2021

Inflationary dynamics and particle production in a toroidal Bose-Einstein condensate

Anshuman Bhardwaj
Louisiana State University

Dzmitry Vaido
Louisiana State University

Daniel E. Sheehy
Louisiana State University

Follow this and additional works at: https://digitalcommons.lsu.edu/physics_astronomy_pubs

Recommended Citation

Bhardwaj, A., Vaido, D., & Sheehy, D. (2021). Inflationary dynamics and particle production in a toroidal Bose-Einstein condensate. *Physical Review A, 103* (2) https://doi.org/10.1103/PhysRevA.103.023322

This Article is brought to you for free and open access by the Department of Physics & Astronomy at LSU Digital Commons. It has been accepted for inclusion in Faculty Publications by an authorized administrator of LSU Digital Commons. For more information, please contact ir@lsu.edu.

arXiv:2009.05611v1 [cond-mat.quant-gas] 11 Sep 2020

Inflationary Dynamics and Particle Production in a Toroidal Bose-Einstein Condensate

Anshuman Bhardwaj,[1,*] Dzmitry Vaido,[1,†] and Daniel E. Sheehy[1,‡]

[1] *Department of Physics and Astronomy, Louisiana State University, Baton Rouge, LA 70803 USA*

(Dated: September 11, 2020)

We present a theoretical study of the dynamics of a Bose-Einstein condensate (BEC) trapped inside an expanding toroid that can realize an analogue inflationary universe. As the system expands, we find that phonons in the BEC undergo redshift and damping due to quantum pressure effects. We predict that rapidly expanding toroidal BEC's can exhibit spontaneous particle creation, and study this phenomenon in the context of an initial coherent state wavefunction. We show how particle creation would be revealed in the atom density and density correlations, and discuss connections to the cosmological theory of inflation.

I. INTRODUCTION

The theory of inflation is the most promising description of the early universe [1–7], although alternatives exist [8]. This theory is based on a field ϕ, the inflaton, propagating in a classical spacetime and moving under the influence of its own potential $V(\phi)$. The quantum fluctuations in the inflaton field couple with the spatial curvature of the universe, thus acting as seeds for the observed cosmic microwave background (CMB) anisotropies [9] and the large scale structure of our universe [10], although primordial gravitational waves are yet to be observed. The exact shape of the potential $V(\phi)$ is currently not known, although work has been done to reconstruct it [11]. Indeed, experiments have put stringent constraints on some of the candidates such as the quadratic and quartic inflationary potentials, though there remains a huge class of models that are able to explain observations [12]. In addition, the CMB observations have revealed possible anomalies on the largest scales with a 3σ significance, that hint towards new physics [13]. However, testing inflationary models using cosmological experiments is expensive and difficult.

A natural question, then, is if there exists an alternative setting to test the predictions of inflation. The answer is 'Analogue Gravity' [14], where the aim is to come up with simple experimental setups that can be performed in a lab and which mimic the equations governing gravitational and cosmological phenomena such as inflation and black hole physics. Early work in this direction came from Unruh who, in 1981, showed [15] that the Navier-Stokes' equations for fluid flow, such as in a draining bathtub, could mimic Hawking radiation [16, 17] coming from a black hole horizon. This showed that analogue black holes can be constructed, allowing the study of near-horizon physics outside of an astrophysical setting. Several recent experiments have confirmed the existence of such analogue Hawking radiation [18–21], as well as other phenomena such as classical superradiance [22], the Casimir effect [23], and Sakharov oscillations [24]. Other analogue gravity proposals test ideas like the Gibbons-Hawking effect [25], the vacuum decay [26–29] and the Unruh effect [30].

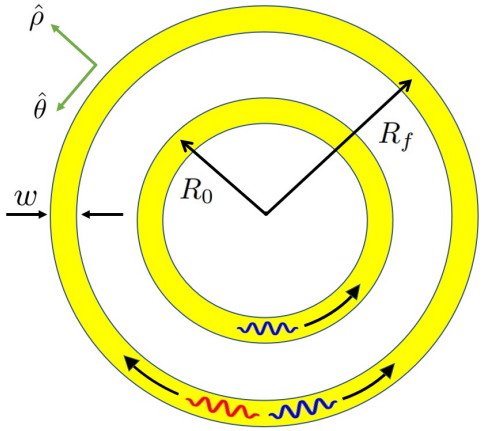

Figure 1: (Color Online) Sketch of the initial (with radius R_0) and final (with radius R_f) state of an expanding ring-shaped (toroidal) BEC, as realized in Ref. 38. As depicted, an initial density wave traveling counterclockwise (*blue*) bifurcates due to phonon creation, into two counter propagating waves (*red and blue*). In the main text, we use polar coordinates (ρ, θ, z) with with z directed out of the page. We also indicated the ring diameter w, implying that the ring cross-sectional area $\mathcal{A} \simeq \frac{1}{4}\pi w^2$ for the case of a circular cross section. However, in the main text we shall allow for different radii in the ρ and z direction (denoted by R_ρ and R_z, respectively).

Inflation in analogue systems has been studied theoretically [31–37], and realized experimentally in Bose-Einstein condensates (BECs) [38] and in ion traps [39]. Here, our primary motivation is the BEC implementation of analogue inflation realized by Eckel et al [38]. The Eckel et al experiments featured a BEC in a time-dependent trap with the shape of a thin toroid, with a rapid expansion of the toroid mimicking the inflationary era. Some of the analogues of cosmological phenomena

*Electronic address: abhard4@lsu.edu
†Electronic address: dvaido1@lsu.edu
‡Electronic address: sheehy@lsu.edu

observed by Eckel et al were the red-shifting of frequencies and damping of modes due to expansion. Vortex creation after halting of the ring expansion was also observed, an analogue of reheating in the early universe.

In this paper, we present analytical results to help understand the Eckel et al experiments and discuss other possible observables that can probe inflationary physics in the context of an analogue BEC experiment. The rest of the paper is organized as follows: in Sec. II , we investigate the evolution of perturbations (i.e., phonons) in a BEC using the Bogoliubov-de Gennes Hamiltonian. In Sec. III, we show that this approach leads to the Mukhanov-Sasaki equation [40–42] that governs evolution of such phonons in the primordial universe. This equation forces the density fluctuations to undergo damping that comes from quantum pressure. In Sec. IV, we show that as the ring undergoes an expansion there is a spontaneous generation of phonons which is the analogue of particle creation in the early universe. In Sec. V, we study the case of stimulated phonon creation by calculating the average density in a coherent state and showing that an initial traveling density wave bifurcates (due to phonon creation) into two waves, as illustrated in Fig. 1. In Sec. VI, we calculate the density-density correlation function for this system, showing that the angle-dependence of density correlations exhibits a signature of phonon production. In Sec. VII, we provide brief concluding remarks and in Appendix A we provide details that are omitted from the main text.

II. BOGOLIUBOV-DE GENNES HAMILTONIAN

In this section we describe, within the Bogoliubov-de Gennes (BdG) formalism, how a boson gas in a time-dependent trap can exhibit emergent relativistic dynamics that mimic the phenomenon of inflation. We start with the following Hamiltonian that describes a Bose-Einstein condensate (BEC), given in terms of a complex scalar field ($\hat{\Phi}(\boldsymbol{r})$), evolving inside a non-uniform and time dependent toroidal potential $V(\boldsymbol{r},t)$:

$$\begin{aligned}\hat{H} &= \hat{H}_0+\hat{H}_1,\\ \hat{H}_0 &= \int d^3r\ \hat{\Phi}^\dagger(\boldsymbol{r})\Big[-\frac{\hbar^2}{2M}\nabla^2+V(\boldsymbol{r})-\mu\Big]\hat{\Phi}(\boldsymbol{r}),\\ \hat{H}_1 &= \frac{U}{2}\int d^3r\ \hat{\Phi}^\dagger(\boldsymbol{r})\hat{\Phi}^\dagger(\boldsymbol{r})\hat{\Phi}(\boldsymbol{r})\hat{\Phi}(\boldsymbol{r}),\end{aligned} \tag{1}$$

where μ is the chemical potential, $U=\frac{4\pi a_s\hbar^2}{M}$ is the interaction parameter, a_s is the scattering length, $\hbar$ is Planck's constant, and M is the mass of the bosonic atoms. The time-dependent single-particle potential $V(\boldsymbol{r},t)$ describes a time-dependent toroidal potential which, taking a cylindrical coordinate system $\boldsymbol{r}=(\rho,\theta,z)$, we can take to be parabolic in the $\hat{z}$ direction and a higher power law in the radial ($\hat{\rho}$) direction:

$$V(\boldsymbol{r},t)=\frac{1}{2}M\omega_z^2z^2+\lambda|\rho-R(t)|^n, \tag{2}$$

consistent with the experiments of Eckel et al [38], who realize a "flat bottomed" trap with the exponent $n\simeq 4$. Here, $R(t)$ is the externally-controlled radius of the toroid that increases with time. The condensate field operator obeys the commutation relation

$$\big[\hat{\Phi}(\boldsymbol{r}),\hat{\Phi}^\dagger(\boldsymbol{r'})\big]=\delta^{(3)}(\boldsymbol{r}-\boldsymbol{r'}). \tag{3}$$

Under the BdG approximation, the condensate field operator in the Heisenberg picture $\hat{\Phi}(\boldsymbol{r},t)$ can be written as the sum of a coherent background $\Phi_0(\boldsymbol{r},t)$ and the perturbation operator $\delta\hat{\phi}(\boldsymbol{r},t)$:

$$\hat{\Phi}=\Phi_0(1+\delta\hat{\phi}). \tag{4}$$

Plugging Eq. (4) into the Hamiltonian (1) and using Heisenberg's equations of motion, we get

$$i\hbar\partial_t\delta\hat{\phi}=-\frac{\hbar^2}{2M}\nabla^2\delta\hat{\phi}-\frac{\hbar^2}{M}\frac{\boldsymbol{\nabla}\Phi_0}{\Phi_0}\cdot\boldsymbol{\nabla}\delta\hat{\phi}+Un_0\big[\delta\hat{\phi}^\dagger+\delta\hat{\phi}\big], \tag{5}$$

for the $\delta\hat{\phi}(\boldsymbol{r},t)$ equation of motion [36]. Here, we defined the background density as $n_0(\boldsymbol{r},t)\equiv|\Phi_0(\boldsymbol{r},t)|^2$.

Equation (5) describes dynamics of the perturbation operator $\delta\hat{\phi}$ in the presence of a time-dependent background $\Phi_0(\boldsymbol{r},t)$. Below, we find it convenient to transform to the Madelung representation in terms of density $\hat{n}(\boldsymbol{r},t)$ and phase $\hat{\phi}(\boldsymbol{r},t)$ field operators via:

$$\hat{\Phi}(\boldsymbol{r},t)=\sqrt{\hat{n}(\boldsymbol{r},t)}e^{i\hat{\phi}(\boldsymbol{r},t)}. \tag{6}$$

To proceed we use Eq. (4) on the left hand side of Eq. (6) and we introduce linear perturbations for the phase $\hat{\phi}=\phi_0+\hat{\phi}_1$ and the density $\hat{n}=n_0+\hat{n}_1$ on the right hand side of Eq. (6). Then, keeping first-order contributions, we obtain an expression for the condensate perturbation $\delta\hat{\phi}$ in terms of the perturbations in density $\hat{n}_1(\boldsymbol{r},t)$ and phase $\hat{\phi}_1(\boldsymbol{r},t)$:

$$\delta\hat{\phi}(\boldsymbol{r},t)\ =\ \frac{\hat{n}_1(\boldsymbol{r},t)}{2n_0(\boldsymbol{r},t)}+i\hat{\phi}_1(\boldsymbol{r},t). \tag{7}$$

Here $\phi_0(\boldsymbol{r},t)$ denotes the background phase. The phase and density perturbations satisfy the commutation relation $\big[\hat{n}_1(\boldsymbol{r},t),\hat{\phi}_1(\boldsymbol{r'},t)\big]=i\delta^{(3)}(\boldsymbol{r}-\boldsymbol{r'})$. Substituting the above relation into (5) and using Madelung's representation for the background $\Phi_0(\boldsymbol{r},t)=\sqrt{n_0(\boldsymbol{r},t)}e^{i\phi_0(\boldsymbol{r},t)}$, we get the equations of motion for the phase and density perturbations [38]:

$$-\frac{\hbar}{U}\partial_t\hat{\phi}_1\ =\ \hat{\mathcal{D}}\hat{n}_1+\frac{\hbar^2}{MU}\boldsymbol{\nabla}\phi_0\cdot\boldsymbol{\nabla}\hat{\phi}_1, \tag{8}$$

$$\partial_t\hat{n}_1\ =\ -\frac{\hbar}{M}\boldsymbol{\nabla}\cdot\Big[\hat{n}_1\boldsymbol{\nabla}\phi_0+n_0\boldsymbol{\nabla}\hat{\phi}_1\Big], \tag{9}$$

where we made use of the continuity equation for n_0: $\partial_tn_0=-\frac{\hbar}{M}\boldsymbol{\nabla}\cdot\big(n_0\boldsymbol{\nabla}\phi_0\big)$ and we defined the operator

$$\hat{\mathcal{D}}\equiv 1-\frac{\hbar^2}{2MU}\Big(\frac{\nabla^2}{2n_0}-\frac{\boldsymbol{\nabla}n_0\cdot\boldsymbol{\nabla}}{2n_0^2}-\frac{\nabla^2n_0}{2n_0^2}+\frac{(\boldsymbol{\nabla}n_0)^2}{2n_0^3}\Big). \tag{10}$$

The terms in parentheses in $\hat{\mathcal{D}}$ are due to the quantum pressure, which are often neglected in the hydrodynamic limit where $\hat{\mathcal{D}} \approx 1$. In that situation, Eqs. (8) and (9) can be readily combined to get a relativistic wave equation for $\hat{\phi}_1$ (see [34, 35, 38]) :

$$0 = \frac{1}{\sqrt{-g}}\partial_\mu(\sqrt{-g}g^{\mu\nu}\partial_\nu\hat{\phi}_1), \tag{11}$$

where $\mu = 0$ denotes time and $\mu = 1, 2, 3$ denote space so $x^\mu = (ct, x, y, z)$ and $\partial_\mu = (\frac{1}{c}\frac{\partial}{\partial t}, \boldsymbol{\nabla})$ where $c = \sqrt{Un_0/M}$ is the BEC speed of sound. Here, the metric is

$$g_{\mu\nu} = \begin{bmatrix} -c^3 & 0 & 0 & 0 \\ 0 & c(R+\tilde{\rho})^2 & 0 & 0 \\ 0 & 0 & c & 0 \\ 0 & 0 & 0 & c \end{bmatrix}, \tag{12}$$

with determinant $g = -c^6(R+\tilde{\rho})^2$, where $\tilde{\rho} = \rho - R(t)$ is the comoving radial coordinate.

Equation (11) shows that a boson gas in a time-dependent toroidal trap indeed simulates an expanding one-dimensional universe with the metric Eq. (12). However, below we show that although the quantum pressure terms in $\hat{\mathcal{D}}$ are small, their inclusion qualitatively impacts the dynamics of low-energy modes in the expanding toroidal BEC, leading to damping and spontaneous phonon creation.

Having obtained equations (8) and (9), that describe excitations of a superfluid boson gas in a time-dependent trap, in the next section we show how, in the thin-ring limit, these equations reduce to the Mukhanov-Sasaki equation that describes damped sound modes.

III. THE MUKHANOV-SASAKI EQUATION

Equations (8) and (9) derived in the preceding section describe phase and density perturbations (i.e., phonons) in a BEC with a generic time-dependent trapping potential $V(\boldsymbol{r}, t)$. In fact, the potential $V(\boldsymbol{r}, t)$ only explicitly appears in the dynamics of the background density (n_0) and phase (ϕ_0) on which phonons propagate (which we study in Appendix A), while the density and phase perturbations $\hat{n}_1$ and $\hat{\phi}_1$ are sensitive to n_0 and ϕ_0 via Eqs. (8) and (9). Our first task is to make simplifying approximations that apply to the geometry realized in Ref. 38, i.e., a thin expanding toroidal trapping potential. As we shall see, this leads to the Mukhanov-Sasaki equation for damped sound modes.

The first simplifying approximation we shall invoke is to neglect the ρ and z dependences of the phase and density perturbations, thereby replacing $\hat{\phi}_1(\boldsymbol{r}, t) \to \hat{\phi}_1(\theta, t)$ and $\hat{n}_1(\boldsymbol{r}, t) \to \mathcal{V}^{-1}\hat{n}_1(\theta, t)$ in Eqs. (8) and (9), where $\mathcal{V} = R\mathcal{A}$ is a volume scale with $\mathcal{A}$ the cross-sectional area of the toroid (so that $2\pi\mathcal{V}$ is the toroid volume). We note that the angle-dependent density fluctation operator $\hat{n}_1(\theta)$ is dimensionless.

Such an approximation holds in the thin-ring limit, where the toroidal radius $R(t)$ is much larger than the typical length scales R_ρ and R_z (defined in Appendix A) characterizing the ring cross-sectional area (see Fig. 1). This implies that an initial angle-dependent perturbation around the ring, such as prepared in the experiments of Ref. [38], will not excite density variations in the ρ and z directions.

The second simplifying approximation we shall invoke is to assume that the background phase ϕ_0 and density n_0 are functions only of ρ and z (i.e., they are independent of θ). This is expected, given the angular symmetry of the toroidal trapping potential. We shall furthermore assume that the condensate and the ring are moving with the same velocity, i.e., the superfluid velocity equals the ring velocity $\boldsymbol{v} = \frac{\hbar}{M}\boldsymbol{\nabla}\phi_0 = \dot{R}\hat{\rho}$ (here $\dot{R} \equiv \frac{dR}{dt}$). The conditions for validity of this assumption are explored in Appendix A. This implies that the gradients in the perturbations are orthogonal to the condensate velocity i.e. $\boldsymbol{v}\cdot\boldsymbol{\nabla}\hat{\phi}_1 = \boldsymbol{v}\cdot\boldsymbol{\nabla}\hat{n}_1 = 0$. By a similar argument, the dot-product term $\boldsymbol{\nabla}n_0\cdot\boldsymbol{\nabla}\hat{n}_1 = 0$ in the quantum pressure also vanishes. On the other hand the divergence of condensate velocity is not zero: $\boldsymbol{\nabla}\cdot\boldsymbol{v} = \frac{\hbar}{M}\nabla^2\phi_0 \approx \frac{\dot{R}}{R}$.

Within these approximations, the equations of motion (8) and (9) in the thin ring limit take the form:

$$-\frac{\hbar\mathcal{V}}{U}\partial_t\hat{\phi}_1(\theta, t) = \hat{\mathcal{D}}_\theta\hat{n}_1(\theta, t), \tag{13}$$

$$\partial_t\hat{n}_1(\theta, t) = -\frac{\dot{R}}{R}\hat{n}_1(\theta, t) - \frac{\hbar\mathcal{V}n_0}{MR^2}\partial_\theta^2\hat{\phi}_1(\theta, t), \tag{14}$$

describing angle-dependent excitations in a thin radially expanding toroidal BEC. Here $\hat{\mathcal{D}}_\theta \equiv 1 - \frac{\hbar^2}{2MU}\left(\frac{\partial_\theta^2}{2n_0R^2} - \frac{\nabla^2 n_0}{2n_0^2} + \frac{(\boldsymbol{\nabla}n_0)^2}{2n_0^3}\right)$ is the projection of $\hat{\mathcal{D}}$ in the θ-space. To solve this system of equations, we introduce mode expansions as :

$$\hat{\phi}_1(\theta, t) = \sqrt{\frac{U}{2\pi\mathcal{V}\hbar}}\sum_{n=-\infty}^{\infty}\left[e^{in\theta}\chi_n(t)\hat{a}_n + e^{-in\theta}\chi_n^*(t)\hat{a}_n^\dagger\right], \tag{15}$$

$$\hat{n}_1(\theta, t) = \sqrt{\frac{U\mathcal{V}}{2\pi\hbar}}\sum_{n=-\infty}^{\infty}\left[e^{in\theta}\eta_n(t)\hat{a}_n + e^{-in\theta}\eta_n^*(t)\hat{a}_n^\dagger\right], \tag{16}$$

where the ladder operators $\hat{a}_n$ satisfy $\left[\hat{a}_n, \hat{a}_{n'}^\dagger\right] = \delta_{n,n'}$, and the mode functions are assumed to be same whether the modes are traveling clockwise or anticlockwise, i.e. $\chi_{-n} = \chi_n$ and $\eta_{-n} = \eta_n$. We take $\chi_n(t)$ and $\eta_n(t)$ to satisfy $(\eta_n\chi_n^* - \eta_{-n}^*\chi_{-n}) = i\hbar/U$, which leads to the commutation relation $\left[\hat{n}_1(\theta, t), \hat{\phi}_1(\theta', t)\right] = i\delta(\theta - \theta')$. Substituting these mode expansions in (13) and (14), we get the following equations of motion for the mode functions:

$$-\frac{\hbar}{U}\dot{\chi}_n(t) = D_n\eta_n(t), \tag{17}$$

$$\dot{\eta}_n(t) = -\frac{\dot{R}}{R}\eta_n + \frac{\hbar n_0}{MR^2}n^2\chi_n, \tag{18}$$

where $D_n \equiv 1+\frac{\hbar^2}{4M^2c^2}\left(\frac{n^2}{R^2}+\frac{\nabla^2 n_0}{n_0}-\frac{(\nabla n_0)^2}{n_0^2}\right)$ is the eigenvalue of $\hat{\mathcal{D}}_\theta$.

To arrive at the Mukhanov-Sasaki equation, we eliminate η_n in favor of χ_n:

$$\ddot{\chi}_n + \left(1+\gamma_{\rm QP}\right)\frac{\dot{R}}{R}\dot{\chi}_n + \alpha_{\rm QP}\frac{n^2c^2}{R^2}\chi_n = 0. \qquad (19)$$

The corrections due to quantum pressure are $\gamma_{\rm QP} = -\frac{R}{\dot{R}}\cdot\frac{\dot{D}_n}{D_n}$ and $\alpha_{\rm QP} = D_n$. In general these are dependent on density, radius of the ring and the mode index n. However, we can make an estimate of what values these corrections typically take. We start by approximating the density gradient $\boldsymbol{\nabla} n_0$ by the density divided by the width of the ring w (characterized by the TF radii R_ρ and R_z, see Appendix A). Similarly, we can approximate $\nabla^2 n_0 \simeq -n_0/w^2$. Thus $D_n \approx 1+\frac{n^2}{2}\left(\frac{\xi}{R}\right)^2-\left(\frac{\xi}{w}\right)^2$, where $\xi = \frac{\hbar}{\sqrt{2}Mc}$ is the coherence length. In the hydrodynamic limit, where the coherence length is small compared to the dimensions of the ring, $\alpha_{QP} = D_n \approx 1$.

To estimate $\gamma_{\rm QP}$, we need to estimate $\dot{D}_n$. To do this we use experimental parameters from Ref. 38, with M given by the mass of a ^{23}Na atom, the speed of sound $c \approx 2$ mm/s and the width of the ring $w \approx 2$ μm (which is indeed an order of magnitude smaller than the radius $R(t)$ that varies between 10 μm to 50 μm [38]). Thus $\left(\frac{\xi}{w}\right)^2 \approx 10^{-1}$. Also, since the width of the ring is small compared to its radius, $w \ll R(t)$, we find $\dot{D}_n \approx -\frac{1}{2}\left(\frac{\xi}{w}\right)^2\frac{\dot{R}}{R}$. Here we estimate the ring width via $w = \sqrt{\frac{2\mu}{M\omega_z^2}}$, where ω_z is the trapping frequency in the z direction. We also made use of the local density approximation (LDA) to estimate the chemical potential in a harmonic trap. Following [38], we get $\mu \propto R^{-1/2}$ (see Appendix A). This implies that $\gamma_{\rm QP} \approx \frac{1}{2}\left(\frac{\xi}{w}\right)^2 \approx 10^{-1}$.

The preceding arguments suggest a natural approximation for (19) in which we take $\alpha_{\rm QP} \to 1$ and $\gamma_{\rm QP} \to 0$. Indeed, this approximation brings Eq. (19) into a very simple form:

$$\ddot{\chi}_n + \frac{\dot{R}}{R}\dot{\chi}_n + \frac{n^2c^2}{R^2}\chi_n = 0, \qquad (20)$$

where we assume a constant speed of sound c. This form was discussed in detail in [38], and is expected to hold for a one dimensional universe. To solve this, we introduce the conformal time $d\eta = \frac{cdt}{R(t)}$ that measures the horizon size in cosmology. Equation (20) then takes the form of a simple harmonic oscillator: $\chi_n''(\eta) + n^2\chi(\eta) = 0$, with plane waves $e^{\pm i|n|\eta}$ as solutions. Thus switching back to proper time t we get :

$$\chi_n(t)\Big|_{\gamma=0} \sim \exp\left[\pm i|n|\int_0^t \frac{cdt'}{R(t')}\right]. \qquad (21)$$

This shows that the amplitude of the modes will be conserved with time in the $\gamma_{\rm QP} \to 0$ limit. Thus the quantum pressure correction $\gamma_{\rm QP}$ plays the role of a damping parameter. As we will see in Sec. IV, nonzero $\gamma_{\rm QP}$ (even if it is small in magnitude) is essential for particle production.

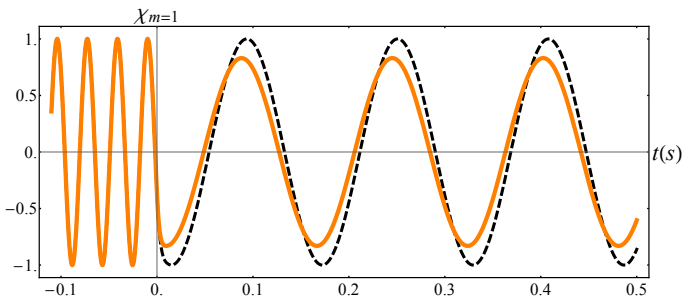

Figure 2: (Color Online) Comparison of solutions χ_m of (22) for $m = 1$ mode without quantum pressure ($\gamma = 0$) (*dashed, black*) and with quantum pressure ($\gamma = 0.5$) (*solid, orange*) (for $t < 0$ they coincide). The modes undergo damping and redshift just as they do in the inflationary era. For this plot, we took the speed of sound to be $c = 2$ mm/s, the initial radius to be $R_0 = 10\mu$m, the timescale that governs the expansion of the ring to be $\tau = 6.21$ms and the duration of expansion to be $t_f = 10$ms.

Thus, while small, the quantum pressure correction represented by $\gamma_{\rm QP}$ fundamentally modifies the solutions of the Mukhanov-Sasaki equation. In general, the parameters $\gamma_{\rm QP}$ and $\alpha_{\rm QP}$ are dependent on time, but in what follows, we will assume them to be constants ($\gamma_{\rm QP} = \gamma$, $\alpha_{\rm QP} = \alpha$). This approximation gives us an analytic handle on the parameter space, where the basic physical features like the particle creation can be modeled without going in to the fine details of how they evolve with time. We will take γ to be a small number and take $\alpha \to 1$ as its sole purpose is to slightly shift the frequency of the modes without affecting the damping and thus it has no role in particle creation. Within these approximations, (19) reduces to the following Mukhanov-Sasaki equation [40–42]:

$$\ddot{\chi}_n + \left(1+\gamma\right)\frac{\dot{R}}{R}\dot{\chi}_n + \frac{n^2c^2}{R^2}\chi_n = 0, \qquad (22)$$

where we have assumed the speed of sound c to be a constant.

In the following, we also choose a specific form for the time-dependent radius $R(t)$. Our choice is motivated by the fact that, in the inflationary era, the Hubble parameter $H \equiv \frac{\dot{a}}{a} \approx H_0$ is roughly a constant and one could model this phase with a de-Sitter type inflation where the scale factor $a(t) \sim e^{H_0 t}$ [43, 44]. This motivates us to study an exponential expansion $R(t) = R_0 e^{t/\tau}$ of the ring radius, characterized by the timescale τ. Then the general solution to Eq. (22) is:

$$\chi_n(t) = e^{-\frac{t}{2\tau}(1+\gamma)}\left[A_n J_{\frac{1+\gamma}{2}}(z) + B_n J_{-\frac{1+\gamma}{2}}(z)\right], \qquad (23)$$

where the time dependent parameter $z = \omega_n\tau$ with the

frequency $\omega_n = \frac{|n|c}{R(t)}$ and $J_n(z)$ are Bessel functions of the first kind. The coefficients A_n and B_n are fixed by the initial conditions.

To illustrate the effect of nonzero γ in the case of exponential inflation in the toroid, in Fig. 2 we plot χ_n as a function of t for an $n = 1$ mode for the case of $\gamma = 0$ (dashed curve) and $\gamma = 0.5$ (solid curve). For $t < 0$ (before expansion), both curves show oscillatory motion, and during expansion (for $t > 0$), where they are governed by Eq. (23), they both show a redshift [38] i.e. their frequency $\omega_n = \frac{nc}{R(t)}$ decreases as the ring expands. However, while the $\gamma = 0$ curve shows no reduction of amplitude, the $\gamma = 0.5$ curve exhibits damping due to quantum pressure. Both of these phenomena, the redshift and damping, have their respective counterparts in cosmology.

Before concluding this section, we note that, as in conventional inflationary theory, the fate of modes after expansion in a toroidal BEC is strongly dependent on the mode index n (which controls the mode wavelength). To see this, note that for exponential expansion $R(t) \propto e^{t/\tau}$, the horizon size is given by $\eta_{\rm H} = \int_0^{t_f} \frac{cdt}{R(t)} = c\tau(1 - e^{-t_f/\tau})$. After the expansion persists long enough i.e. t_f/τ is large, then the horizon size is $\eta_{\rm H} \sim c\tau$. If the parameter $z = \frac{|n|c\tau}{R(t)}$ is small, i.e., $\frac{R}{|n|} \gg c\tau$, then the wavelengths of the modes are much larger than the horizon size and the mode solution (23) becomes constant in time:

$$\chi_n(t) \approx \left(\frac{2R_0}{|n|c\tau}\right)^{\frac{1+\gamma}{2}} \frac{B_n}{\Gamma\left(\frac{1-\gamma}{2}\right)}, \tag{24}$$

where we have used the result that for small arguments $z \to 0$, the Bessel function goes as $J_n(z) \to \frac{1}{\Gamma(n+1)}\left(\frac{z}{2}\right)^n$. This freezing of super-horizon modes (i.e. with small mode index) is a very important aspect of the inflationary mechanism as these modes re-enter the horizon at a later time and form large scale structures in the observable universe. In the next section, we will discuss how phonons are produced due to the mode solution (23) and see the importance of the super-horizon modes in the expanding ring.

IV. SPONTANEOUS PHONON CREATION

Now that we have solved the Mukhanov-Sasaki equation for a constant quantum pressure parameter γ, in this section we use its solution (23) to understand how a BEC in the vacuum state, when expanded exponentially, will exhibit the dynamical generation of phonons. We start with an initially static BEC in its vacuum state. The mode functions for this initial BEC (which we denote as the "in" state) obey Eq. (22), but with $\dot{R} = 0$ (so that they are undamped). These inital mode functions are:

$$\chi_n^{\rm in}(t) = \frac{1}{\sqrt{2\omega_n^0}} e^{-i\omega_n^0 t}, \tag{25}$$

which satisfy $i\partial_t \chi_n^{\rm in} = \omega_n^0 \chi_n^{\rm in}$, where ω_n^0 is the frequency at $t = 0$. These positive-frequency 'in'-mode functions satisfy the Wronskian condition $W[\chi_n, \chi_n^*] = \dot{\chi}_n \chi_n^* - \chi_n \dot{\chi}_n^* = -i$, and associated with them is the structure of ladder operators $\hat{a}_n$ that annihilate their associated 'a-vacuum' state: $\hat{a}_n|0_a\rangle = 0$.

Having described the normal modes of the initial BEC, we turn to the impact of a period of exponential growth on the BEC, starting at $t = 0$, and described by the exponential function $R(t) = R_0 e^{t/\tau}$. During this period, the modes evolve according to (23), where the coefficients are fixed by matching the mode functions $\chi_n(t)$ and their time derivatives with that of the initial BEC at $t = 0$. This matching results in the conditions:

$$\begin{aligned} A_n &= \frac{J_{\frac{1-\gamma}{2}}(z_0) + iJ_{-\frac{1+\gamma}{2}}(z_0)}{J_{\frac{1+\gamma}{2}}(z_0)J_{\frac{1-\gamma}{2}}(z_0) + J_{-\frac{1+\gamma}{2}}(z_0)J_{\frac{-1+\gamma}{2}}(z_0)}, \\ B_n &= \frac{J_{\frac{-1+\gamma}{2}}(z_0) - iJ_{\frac{1+\gamma}{2}}(z_0)}{J_{\frac{1+\gamma}{2}}(z_0)J_{\frac{1-\gamma}{2}}(z_0) + J_{-\frac{1+\gamma}{2}}(z_0)J_{\frac{-1+\gamma}{2}}(z_0)}, \end{aligned} \tag{26}$$

where $z_0 = \frac{|n|c\tau}{R_0}$. Equation (23), along with these coefficients, describes the mode functions during the exponential growth regime of the toroidal BEC.

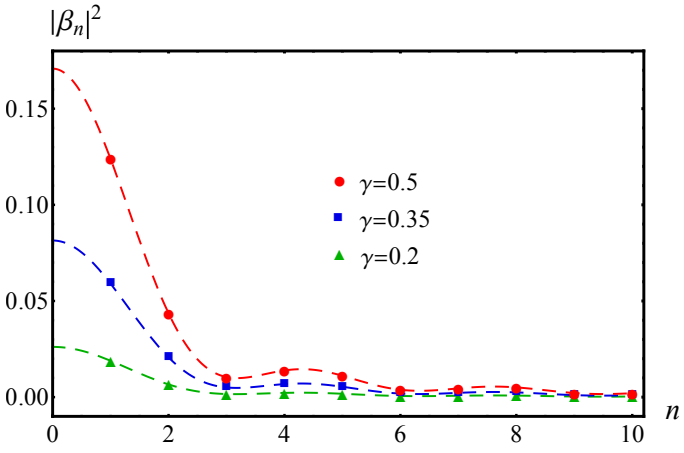

Figure 3: (Color Online) The particle production parameter $|\beta_n|^2$ as function of mode index n for various values of the quantum pressure $\gamma = 0.2$ (*green*), $\gamma = 0.35$ (*blue*) and $\gamma = 0.5$ (*red*). The dashed lines show $|\beta_n|^2$ as continuous functions to emphasize their overall dependence on the discrete mode indices. For this plot, we took the speed of sound to be $c = 2$ mm/s, the initial radius to be $R_0 = 10\mu$m, the expansion timescale to be $\tau = 6.21$ms and the duration of expansion to be $t_f = 10$ms.

The expansion comes to a halt at some later time $t = t_f$. In this third regime, the BEC is again static, with excitations described by 'out'-mode solutions that are analogous to Eq. (25):

$$\chi_n^{\rm out}(t) = \frac{1}{\sqrt{2\omega_n^f}} e^{-i\omega_n^f (t - t_f)}. \tag{27}$$

However, once the expansion ends, the resulting static regime will now have a mode solution that is in a superposition of the 'out'-modes (27) :

$$\chi_n^f(t) = e^{-\frac{t_f}{2\tau}\gamma}\Big[\alpha_n \chi_n^{\rm out}(t) + \beta_n \chi_n^{\rm out*}(t)\Big], \qquad (28)$$

where $\omega_n^f = \frac{|n|c}{R_f}$ is the frequency for $t \geq t_f$. The coefficients in Eq. (28) are obtained by again demanding that the mode function and its derivatives are consistent at t_f, with the $t \to t_f^-$ solution given by Eq. (23) as described above. By solving these matching conditions we find the coefficients α_n and β_n:

$$\alpha_n = \frac{e^{-\frac{t_f}{2\tau}}}{2}\Big[A_n\Big(J_{\frac{1+\gamma}{2}} - iJ_{\frac{-1+\gamma}{2}}\Big) + B_n\Big(J_{-\frac{1+\gamma}{2}} + iJ_{\frac{1-\gamma}{2}}\Big)\Big], \qquad (29)$$

$$\beta_n = \frac{e^{-\frac{t_f}{2\tau}}}{2}\Big[A_n\Big(J_{\frac{1+\gamma}{2}} + iJ_{\frac{-1+\gamma}{2}}\Big) + B_n\Big(J_{-\frac{1+\gamma}{2}} - iJ_{\frac{1-\gamma}{2}}\Big)\Big], \qquad (30)$$

where we have suppressed the arguments of the Bessel functions, which are all evaluated at $z_f = \frac{|n|c\tau}{R_f}$ with R_f the final ring radius. These coefficients, which satisfy $|\alpha_n|^2 - |\beta_n|^2 = 1$, describe the modification of the mode functions χ_n during the expansion process.

The modified mode function (28) in the 'out'-regime, defines a new set of ladder operators $\hat{b}_n$ that annihilate the new 'b-vacuum' state $|0_b\rangle \neq |0_a\rangle$: $\hat{b}_n|0_b\rangle = 0$. The coefficients α_n and β_n provide a Bogoliubov transformation between $\hat{a}_n$ and $\hat{b}_n$ via [45–47]:

$$\hat{a}_n = \alpha_n^* \hat{b}_n - \beta_n^* \hat{b}_{-n}^\dagger, \qquad (31)$$

$$\hat{b}_n = \alpha_n \hat{a}_n + \beta_n^* \hat{a}_{-n}^\dagger. \qquad (32)$$

Thus, if we start with the 'a-vacuum' that has no particles $\langle 0_a|\hat{n}^a|0_a\rangle = 0$, then after going through an expansion phase, the 'b-vacuum' will be bubbling with 'a-particles' [48]. This implies that $\langle 0_b|\hat{n}^a|0_b\rangle = |\beta_n|^2$ where we have defined the number operator $\hat{n}^a = \hat{a}_n^\dagger \hat{a}_n$. This is known as spontaneous particle creation from the vacuum state, characterized by the power parameter $|\beta_n|^2$ that we plot in Fig. 3 with respect to the mode index n, for three values of the quantum pressure parameter $\gamma = 0.2$, $\gamma = 0.35$ and $\gamma = 0.5$.

We now describe the connection of these results to the theory of inflation. We can infer from Fig. 3 that the power associated with small mode indices such as $n = 1$ is much higher than those at larger n. As in inflationary cosmology, this is because during the expansion some modes such as $n = 1$ become super-horizon and freeze (24), i.e. their power remains constant. In contrast, modes that are well within the horizon (i.e., at higher n, or smaller wavelength) are strongly damped and thus their power $|\beta_n|^2$ is reduced.

Thus, larger values of the quantum pressure parameter lead to stronger damping of modes (22) as well as increased spontaneous phonon production. This suggests that the loss of amplitude is converted into phonon production. However, it may be experimentally challenging to observe these spontaneously created phonons. So in the next section, we will discuss the possibility of observing stimulated creation of phonons from a coherent initial state.

V. STIMULATED PHONON CREATION

Having discussed how phonons can be produced by a BEC that is initially in its vacuum state, we now turn to the possibility of starting with a initial coherent state in the mode N:

$$|\alpha, N\rangle = e^{-\frac{1}{2}|\alpha|^2} e^{\alpha \hat{a}_N^\dagger}|0_a\rangle, \qquad (33)$$

where the complex parameter α is a measure of average number of particles in the coherent state given by $|\alpha|^2$. Physically, such a state represents a macroscopic current-carrying state of the BEC. The states $|\alpha, N\rangle$ are

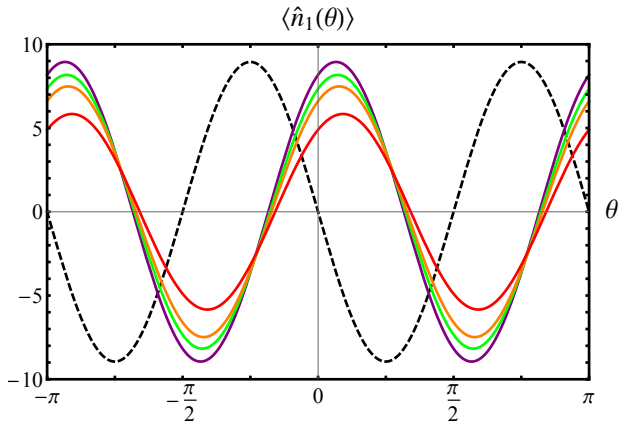

Figure 4: (Color Online) Comparison of average density $\langle \hat{n}_1 \rangle$ before (*dashed, black*) and just after expansion (*solid*) for four values of the quantum pressure parameter γ. In order of decreasing amplitude, the solid curves correspond to $\gamma = 0$ (*violet*), $\gamma = 0.1$ (*green*), $\gamma = 0.2$ (*orange*), and $\gamma = 0.5$ (*red*). Note the $\gamma = 0$ final curve has equal amplitude to the initial density profile (in agreement with our earlier finding shown in Fig. 2), with the phase difference $\alpha_n = e^{i(z_f - z_0)}$ between the curves reflecting the fact that the wave travels around the ring during expansion. For this plot we studied a coherent state characterized by $\alpha = \sqrt{10}$ and mode index $N = 2$. We also took the sound speed to be $c = 2$ mm/s, the initial radius to be $R_0 = 10\mu$m, the timescale for expansion to be $\tau = 6.21$ms and the duration of expansion to be $t_f = 10$ms.

eigenfunctions of the annihilation operators:

$$\hat{a}_m|\alpha, N\rangle = \delta_{m,N}\alpha|\alpha, N\rangle. \qquad (34)$$

In what follows, we will use these coherent states to calculate two observables: the average density in the ring, and (in the next section) the noise correlations, before and after expansion. The advantage of using coherent

states relative to fixed-number Fock states is that in the latter, the average density is zero at all times. This implies that, in an experiment, no significant change will be observed in the average density. For the case of an initial vacuum state, studied in the preceding section, another complication is the presence of other phonon modes, such as thermally excited phonons (since experiments cannot truly reach the zero-temperature vacuum state), that may swamp the signal from spontaneously created phonons. In contrast, in a coherent state, the average densities change with time, making it easier to detect changes due to phonon production.

Since we are in the Heisenberg picture, the system wavefunction is always given by Eq. (33), while the density operators change during the rapid expansion of the ring. We start by writing the mode expansion for the initial density operator (before expansion). To do this, we make use of (16), and the relation (17) between the density η_n and phase χ_n modes neglecting the quantum pressure corrections (i.e. $D_n \approx 1$ here):

$$\hat{n}_1^i(\theta,t) = \mathcal{N}_0 \sum_{n=-\infty}^{\infty} \left[e^{in\theta}\eta_n^{\rm in}(t)\hat{a}_n + e^{-in\theta}\eta_n^{\rm in*}(t)\hat{a}_n^\dagger \right], \tag{35}$$

where $\mathcal{N}_0 = \sqrt{\frac{U\mathcal{V}_0}{2\pi\hbar}}$ is the initial normalization and the 'in'-density modes are $\eta_n^{\rm in}(t) = i\frac{\hbar}{U}\sqrt{\frac{\omega_n^0}{2}}e^{-i\omega_n^0 t}$. Note that we are only neglecting the quantum pressure corrections in the connection between the η_n and χ_n (where they have a small effect) but keeping then in the Mukhanov-Sasaki equaton for the mode functions (where including the quantum pressure is qualitatively important, as we have discussed).

Next, we write down the final density operator after expansion, which has a similar form, but with the 'out'-mode density operators discussed above (see Eqs. (31) and (32))

$$\hat{n}_1^f(\theta,t) = \mathcal{N}_f e^{-\frac{t_f}{2\tau}\gamma} \sum_{n=-\infty}^{\infty} \left[e^{in\theta}\eta_n^{\rm out}(t)\hat{b}_n + e^{-in\theta}\eta_n^{\rm out*}(t)\hat{b}_n^\dagger \right], \tag{36}$$

with the final normalization $\mathcal{N}_f = \sqrt{\frac{U\mathcal{V}_f}{2\pi\hbar}}$ and the 'out'-density modes are defined as $\eta_n^{\rm out}(t) = i\frac{\hbar}{U}\sqrt{\frac{\omega_n^f}{2}}e^{-i\omega_n^f(t-t_f)}$. Now we define the average density in the coherent state as:

$$\langle \hat{n}_1(\theta,t)\rangle = \langle \alpha, N|\hat{n}_1(\theta,t)|\alpha,N\rangle. \tag{37}$$

If we take $\alpha \in \mathcal{R}$, then the initial average density can be written as a wave that travels in the counterclockwise direction ($+\hat{\theta}$):

$$\langle \hat{n}_1^i(\theta,t)\rangle = -2\sqrt{|N|}\alpha \cdot \sin\left[N\theta - \frac{|N|c}{R_0}t\right], \tag{38}$$

where we have set the normalization $\sqrt{\frac{\hbar c\mathcal{V}_0}{4\pi U R_0}}$ to unity for simplicity.

The initial atom density (at $t = 0$) according to Eq. (38) is shown in Fig. 4 with a dotted line, describing a counterclockwise traveling density wave (in the $+\hat{\theta}$ direction). However, upon evaluating the density expectation value after expansion, we find that the final average density can be expressed as a sum of two waves representing phonon creation: A counterclockwise wave traveling wave (direction $+\hat{\theta}$) with amplitude $|\alpha_n|$, representing a reduced initial wave, and a smaller clockwise traveling wave (direction $-\hat{\theta}$) with an amplitude of $|\beta_n|$, thus representing the density wave due to newly created phonons:

$$\begin{aligned}\langle \hat{n}_1^f(\theta,t)\rangle &= -2e^{-\frac{t_f}{2\tau}\gamma}|N|^{\frac{1}{2}}\alpha\Bigg(|\alpha_N|\sin\left[N\theta - \frac{|N|c}{R_f}\Delta t + \varphi_\alpha\right] \\ &- |\beta_N|\sin\left[N\theta + \frac{|N|c}{R_f}\Delta t + \varphi_\beta\right]\Bigg),\end{aligned} \tag{39}$$

where we have again set the normalization $\sqrt{\frac{\hbar c\mathcal{V}_f}{4\pi U R_f}}$ to unity. Here, $\Delta t = (t - t_f)$ is the time elapsed after the expansion has ended, and $\varphi_\alpha = {\rm Arg}(\alpha_N)$ and $\varphi_\beta = {\rm Arg}(\beta_N)$ are respectively, the phase associated with the incoming and created particles. The final density wave is shown in Fig. 4 at $t = t_f$, for various values of quantum pressure. In Fig. 5 we show the density vs. angle for increasing values of the elapsed time $\Delta t = (t - t_f)$. The total density is shown as a black solid curve, and the contributions due to the two terms in Eq. (39), i.e., the abovementioned counterclockwise and clockwise contributions, are depicted as blue (rightmoving arrow) and red (leftmoving arrow) dashed curves, respectively. Although these two contributions are not separately measurable, they can be inferred from the time dependence of the density vs. angle, showing a concrete experimentally testable signature of particle production in an initial coherent state.

VI. DENSITY CORRELATIONS

As we have discussed, a rapidly expanding toroidal BEC undergoes a modification of its vacuum, leading to particle production with amplitude β_n. In this section, we show how this is revealed in correlations of the density fluctuations (i.e., noise correlations). To that end, we define the equal-time fluctuation correlations as follows:

$$\mathcal{C}(\theta,\theta') = \langle \hat{n}_1(\theta,t)\hat{n}_1(\theta',t)\rangle - \langle \hat{n}_1(\theta,t)\rangle\langle \hat{n}_1(\theta',t)\rangle, \tag{40}$$

where the averages are being taken with respect to the initial coherent state $|\alpha,N\rangle$ (in the Heisenberg picture). For the static BEC before expansion, we make use of (35) and (38) to calculate the initial noise correlations. Calculation of these averages leads to:

$$\mathcal{C}^i(\theta-\theta') = \mathcal{N}_0^2 \sum_{n=-\infty}^{\infty} |\eta_n^{\rm in}(t)|^2 {\rm e}^{in(\theta-\theta')}. \tag{41}$$

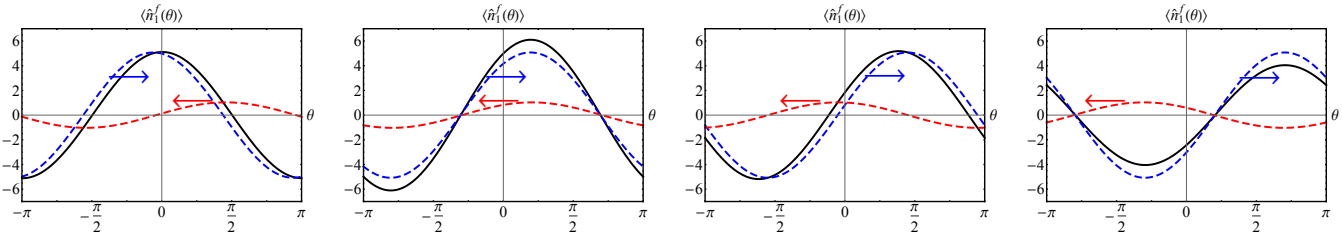

a) $\Delta t = 1.6\tau$ b) $\Delta t = 4.8\tau$ c) $\Delta t = 8.0\tau$ d) $\Delta t = 11.2\tau$

Figure 5: (Color Online) After rapid expansion of the toroidal BEC, an initial traveling wave bifurcates into oppositely-oriented traveling waves, as depicted in Fig. 1. The total density of these waves (*solid, black*), given by Eq. (39), is a sum of a right-moving wave (*dashed, blue, arrow indicating direction*), representing the ingoing particles and a left-moving wave (*dashed, red, arrow indicating direction*) representing the dynamically created particles. For this plot we studied a coherent state characterized by $\alpha = \sqrt{10}$ and mode index $N = 1$, we set the quantum pressure parameter $\gamma = 0.3$, the sound speed to be $c = 2$ mm/s, the initial radius to be $R_0 = 10\mu$m, the duration of expansion to be $t_f = 10$ms and took the timescale governing the trap expansion to be $\tau = 6.21$ms.

Since the mode functions in the summand $|\eta_n^{\rm in}(t)|^2 = \frac{\hbar^2}{2U^2}\omega_n^0 \propto |n|$, this sum is divergent and must be regularized. To implement this regularization, we note that this divergence comes from the fact that we have taken a long-wavelength (low energy) approximation. The linear-in-n energy dependence of these modes must become quadratic, as in the conventional Bogoliubov approximation, for sufficiently large $|n| \geq n_c \equiv \frac{2cMR_0}{\hbar}$. We account for this this by replacing the linear summand with the result following from Bogoliubov theory, which gives:

$$\mathcal{C}^i(\theta-\theta') = \mathcal{N}_0^2 \frac{\hbar^2 c}{2U^2 R_0} n_c \sum_{n=-\infty}^{\infty} \frac{n^2}{\sqrt{n^2(n^2+n_c^2)}} e^{in(\theta-\theta')},$$
$$= \frac{1}{2\pi} n_0 \mathcal{V}_0 \sum_{n=-\infty}^{\infty} \frac{n^2}{\sqrt{n^2(n^2+n_c^2)}} e^{in(\theta-\theta')}, \quad (42)$$

where in the second line we inserted our formulas for $\mathcal{N}_0$, n_c, and c (at the initial radius R_0) to simplify the prefactor. The final sum is convergent, although it has a delta-function piece that we can isolate with the Poisson summation formula to arrive at

$$\mathcal{C}^i(\theta-\theta') = n_0\mathcal{V}_0\Big(\delta(\theta-\theta') + \mathcal{S}(\theta-\theta')\Big), \quad (43)$$

$$\mathcal{S}(\theta) \equiv \frac{1}{2\pi}\sum_{n=-\infty}^{\infty}\Big[\frac{n^2}{\sqrt{n^2(n^2+n_c^2)}} - 1\Big]e^{in\theta}, \quad (44)$$

for the noise correlations before expansion. Similarly, after expansion, the regularized noise correlations take the following form:

$$\mathcal{C}^f(\theta-\theta') = n_0\mathcal{V}_f e^{-\frac{t_f}{\tau}\gamma}\Big(\delta(\theta-\theta')$$
$$+\mathcal{S}(\theta-\theta') + \mathcal{C}^{\rm sub}(\theta-\theta')\Big), \quad (45)$$

where we defined the function

$$\mathcal{C}^{\rm sub}(\theta) \equiv \frac{1}{2\pi}\sum_{n=-\infty}^{\infty}\frac{n^2}{\sqrt{n^2(n^2+n_c^2)}}$$
$$\times 2\Big[|\beta_n|^2 - {\rm Re}\Big(\alpha_n\beta_n^* e^{-2i\omega_n^f\Delta t}\Big)\Big]e^{in\theta}, \quad (46)$$

which, as can be seen by comparing to Eq. (43), is an additional contribution after the rapid expansion of the ring BEC. Here, with the superscript "sub" indicates that this is the subtracted noise correlator, i.e., the difference of the final and initial normalized correlators. Note that this contribution depends on $\Delta t = (t - t_f)$, the time elapsed after expansion, so that the summand exhibits oscillatory behavior as a function of Δt. However, we find that the summand is well approximated by time-averaging over one period $(2\pi/\omega_n)$ of these oscillations, which elimitates the interference term $\alpha_n\beta_n^*$ and yields

$$\mathcal{C}^{\rm sub}(\theta) \simeq \frac{1}{\pi}\sum_{n=-\infty}^{\infty}\frac{n^2}{\sqrt{n^2(n^2+n_c^2)}}|\beta_n|^2 e^{in\theta}, \quad (47)$$

for the subtracted noise correlations.

The expressions (43) and (45) for the initial and final noise correlations have a dirac-delta function that is divergent at $\theta = \theta'$. In plotting these functions, we drop this piece, and set the prefactors (i.e., $n_0\mathcal{V}_0/(2\pi)$ and $n_0\mathcal{V}_f e^{-\frac{t_f}{\tau}\gamma}/(2\pi)$) to unity to simplify comparing the noise before and after expansion. The main part of Fig. 6 shows this comparison, with the initial case being a red dashed line and the final case being a solid green line. We see that each case is dominated by a large (though finite) negative contribution at equal angles ($\theta \to 0$). We regard such anti-correlations as reflecting the repulsion of bosonic atoms at short distances [49, 50]. For larger angular separations, the correlations gradually flatten out [51], except for the appearance of a cusp feature at nonzero angle in the final noise correlations. This cusp clearly represents a signature of the phonon creation, proportional to $|\beta_n|^2$, that we have discussed above. In the inset, we plot the subtracted part Eq. (47) for three values of the quantum pressure parameter: $\gamma = 0.2$ (solid green), $\gamma = 0.35$ (short-dashed blue) and $\gamma = 0.5$ (long-dashed red). This shows that the magnitude of the cusp increases with increasing quantum pressure, although the cusp location is independent of γ. We do find that the

cusp location as a function of angle increases with increasing expansion time t_f, asymptotically approaching $\theta = \pi$ for large t_f.

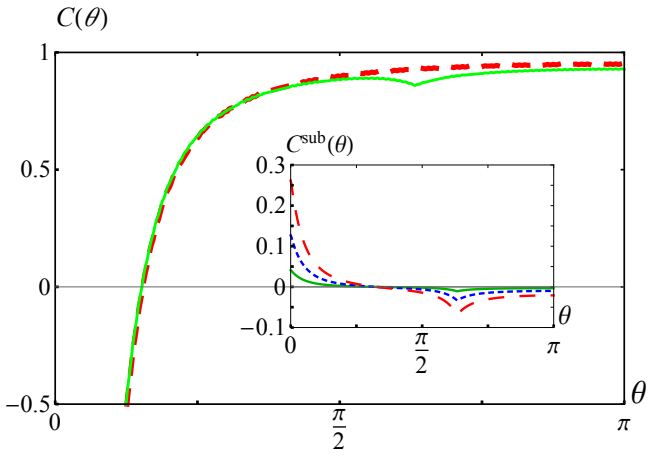

Figure 6: (Color Online) Main: Noise correlations $\mathcal{C}(\theta)$ before (*dashed, red*) given in Eq. (43), and after (*solid, green*) given in Eq. (45)), with quantum pressure $\gamma = 0.5$. In each, we focused on $\theta \neq 0$ (dropping the delta-function piece) and dropped overall prefactors ($\frac{n_0\mathcal{V}_0}{2\pi}$ and $\frac{n_0\mathcal{V}_f}{2\pi}e^{-\frac{t_f}{\tau}\gamma}$, respectively). The correlations after expansion show a cusp like feature that we regard as a signature of particle creation. Inset: To emphasize the cusp, we plot the difference between these curves, the subtracted noise correlations $\mathcal{C}^{\rm sub}(\theta - \theta')$ plotted with respect to the angle difference θ. Here we chose three values of quantum pressure parameter $\gamma = 0.2$ (*solid, green*) and $\gamma = 0.35$ (*short-dashed, blue*) and $\gamma = 0.5$ (*long-dashed, red*). For both plots, we took the speed of sound to be $c = 2$ mm/s, the initial radius to be $R_0 = 10\mu$m, the duration of expansion to be $t_f = 10$ms, the timescale governing the trap expansion to be $\tau = 6.21$ms, and $n_c = 10$.

To better understand the origin of the cusp in Fig. 6, and connect it to particle production during expansion of the ring BEC, we differentiate (47) to get:

$$\frac{d}{d\theta}\mathcal{C}^{\rm sub}(\theta) = -\frac{2}{\pi}\sum_{n=1}^{\infty}\frac{n^2|\beta_n|^2}{\sqrt{n^2+n_c^2}}\sin(n\theta). \qquad (48)$$

A good approximation to this sum results if we Taylor expand the creation parameter β_n for small damping $\gamma \ll 1$ and large mode index $n \gg 1$, which gives $n^2|\beta_n|^2 \approx \left(\frac{\gamma}{4}\right)^2\left(\frac{c\tau}{R_0}\right)^{-2}\left[1 + a^2 - 2a\cos\left(2n\theta_{\rm H}\right)\right]$, where $a = e^{\frac{t_f}{\tau}}$ is the scale factor and $\theta_{\rm H} = \frac{c\tau}{R_0}\left(1 - a^{-1}\right)$ is the angular horizon size at the end of expansion. Upon plugging this into (48), we end up with three sums:

$$\frac{1}{f(\gamma)}\frac{d}{d\theta}\mathcal{C}^{\rm sub}(\theta) = a\sum_{n=1}^{\infty}\frac{\sin(n(\theta - 2\theta_{\rm H}))}{\sqrt{n^2+n_c^2}} + a\sum_{n=1}^{\infty}\frac{\sin(n(\theta + 2\theta_{\rm H}))}{\sqrt{n^2+n_c^2}} - (1+a^2)\sum_{n=1}^{\infty}\frac{\sin(n\theta)}{\sqrt{n^2+n_c^2}}, \qquad (49)$$

where $f(\gamma) = \frac{\gamma^2}{8\pi}\left(\frac{c\tau}{R_0}\right)^{-2}$. For $\theta > 0$, the first sum is the dominant one, and approximating it by an integral we get

$$\sum_{n=1}^{\infty}\frac{\sin(n(\theta - 2\theta_{\rm H}))}{\sqrt{n^2+n_c^2}} \simeq \int_0^{\infty} dx \frac{\sin\left(n_c(\theta - 2\theta_{\rm H})x\right)}{\sqrt{1+x^2}}, \simeq \frac{\pi}{2}\left[\Theta(\theta - 2\theta_{\rm H})I_0\left(n_c(\theta - 2\theta_{\rm H})\right) - L_0\left(n_c(\theta - 2\theta_{\rm H})\right)\right], \qquad (50)$$

where the integration variable $x = n/n_c$, $I_0(x)$ is the modified Bessel function of the first kind, $L_0(x)$ is the modified Struve function and $\Theta(x)$ is the unit step function. The appearance of the latter implies that the derivative is discontinuous at $\theta = 2\theta_{\rm H}$, implying that this determines the position of the cusp as a function of angle. We therefore conclude that the cusp in the correlation function is determined by the angular horizon size:

$$\theta_{\rm cusp} = 2\theta_{\rm H} = 2\frac{c\tau}{R_0}\left(1 - e^{-\frac{t_f}{\tau}}\right). \qquad (51)$$

This result shows that the cusp location is independent of the damping parameter γ, as we saw in Fig. 6. It also explains why the cusp moves away from the origin, eventually slowing down as it approaches $\theta = \pi$, as the duration of expansion t_f increases. The negative correlation at the cusp signifies creation of phonons that anti-bunch as they are created in pairs that move away from each other with opposite momenta [45–47]. This is similar to the 'tongue'-like features that were numerically observed in an acoustic black hole [49]. These results demonstrate that correlations in the density fluctuations show a clear signature of particle production in a rapidly expanding toroidal BEC, showing another signature of inflationary physics.

VII. CONCLUDING REMARKS

In this paper, we have explored how an exponentially expanding thin toroidal Bose-Einstein condensate can reproduce the various features of primordial cosmological inflation. Our work was inspired by recent experimental and theoretical work by Eckel and collaborators who studied inflationary physics in a ring-shaped BEC [38]. These authors observed experimentally (and confirmed theoretically) the redshifting of phonons due to the rapid expansion of this analogue 1D universe, a damping of phonon modes due to Hubble friction, and evidence of the preheating phenomena predicted to occur at the end of inflation.

A central finding of our work is that quantum pressure effects, even if they are quantitatively small, can have important implications for the dynamics of expanding toroidal BEC's. Such quantum pressure effects modify the Mukhanov-Sasaki equations for phonon modes in a fundamental way, with the resulting solutions exhibiting damping and redshift, just like in inflationary cosmology. We found that this damping is responsible for the

change of the vacuum state of the fluctuations, which ultimately leads to the dynamical generation of phonons. This is the analogue of particle production in the early universe. As a result, if the perturbations start in a coherent state, the ring expansion forces them to bifurcate into two density waves that propagate opposite to each other, leading to a complex time-dependent density wave in the toroid. This phonon generation also manifests itself in the density-density noise correlations as a cusp-like feature that tracks the horizon size. Both of these results are clear signatures of particle creation and can be verified experimentally.

Future studies could look into other types of expansion rates like the ones arising from the quadratic or the Starobinsky models of inflation. Another possibility as mentioned in [38], could be to study how causally disconnected regions recombine. This could potentially help cosmology experiments to observe physics beyond our current horizon.

VIII. ACKNOWLEDGEMENTS

The authors are grateful to Ivan Agullo for useful comments. AB acknowledges financial support from the Department of Physics and Astronomy at LSU. DV acknowledges financial support from LSU. DES acknowledges financial support from National Science Foundation Grant No. DMR-1151717.

Appendix A: Dynamics of an expanding toroidal BEC

In this section we study BEC's in the presence of an expanding toroidal-shaped trap given by Eq. (2). Our aim is to understand the background solution on which phonon excitations propagate. For this task we study the time-dependent Gross-Pitaevskii equation (GPE)

$$i\hbar\frac{\partial}{\partial t}\Phi_0(\boldsymbol{r},t) = -\frac{\hbar^2}{2M}\nabla^2\Phi_0(\boldsymbol{r},t) + \big(V(\boldsymbol{r},t)-\mu\big)\Phi_0(\boldsymbol{r},t) + U|\Phi_0(\boldsymbol{r})|^2\Phi_0(\boldsymbol{r},t). \tag{A1}$$

Writing $\Phi_0(\boldsymbol{r},t) = \sqrt{n_0(\boldsymbol{r},t)}\mathrm{e}^{i\phi_0(\boldsymbol{r},t)}$, with n_0 the density and ϕ_0 the superfluid phase, we obtain:

$$-\hbar\partial_t\phi_0(\boldsymbol{r},t) = -\frac{\hbar^2}{2M\sqrt{n_0(\boldsymbol{r},t)}}\nabla^2\sqrt{n_0(\boldsymbol{r},t)} + \frac{\hbar^2}{2M}(\boldsymbol{\nabla}\phi_0(\boldsymbol{r},t))^2 + V(\boldsymbol{r},t) - \mu + Un_0(\boldsymbol{r},t), \tag{A2}$$

$$\partial_t n_0(\boldsymbol{r},t) = -\frac{\hbar}{M}\boldsymbol{\nabla}\cdot\big(n_0(\boldsymbol{r},t)\boldsymbol{\nabla}\phi_0(\boldsymbol{r},t)\big), \tag{A3}$$

A key question is whether the superfluid velocity, $\boldsymbol{v}(\boldsymbol{r},t) = \frac{\hbar}{M}\boldsymbol{\nabla}\phi_0(\boldsymbol{r},t)$, is equal to the radial ring velocity $\hat{\rho}\dot{R}(t)$. Before analyzing this, we recall the simpler case of a *homogeneously translated* trap moving at constant velocity $\boldsymbol{v}_T$. In this case, which can be described by a trapping potential $V(\boldsymbol{r},t) = V(\boldsymbol{r}-\boldsymbol{v}_T t)$, Galilean invariance [52] ensures that a solution to Eqs. (A2) and Eqs.(A3) always exists with superfluid velocity $\boldsymbol{v} = \boldsymbol{v}_T$ and density $n(\boldsymbol{r})$ static in the moving frame.

In the case of present interest, however, a toroidal expanding ring described by the trapping potential Eq. (2), the lack of Galilean invariance means that we cannot find such a simple exact solution with $\boldsymbol{v} = \hat{\rho}\dot{R}(t)$. In the following, we investigate whether such a relation holds approximately under the conditions of the experiment. To do this, we take the gradient of both sides of Eq. (A2), and use the definition of the superfluid velocity, to obtain the Euler equation:

$$-M\partial_t\boldsymbol{v} = \boldsymbol{\nabla}\Big[-\frac{\hbar^2}{2M\sqrt{n_0(\boldsymbol{r},t)}}\nabla^2\sqrt{n_0(\boldsymbol{r},t)} + \frac{1}{2}M\boldsymbol{v}^2 + V(\boldsymbol{r},t) - \mu + Un_0(\boldsymbol{r},t)\Big]. \tag{A4}$$

We now invoke the Thomas-Fermi (TF) approximation [53] by neglecting the Laplacian term in square brackets on the right of Eq. (A4). Then, we plug our assumed solution $\boldsymbol{v} = \hat{\rho}\dot{R}(t)$ into the left side, which leads to $-M\partial_t\boldsymbol{v} = -M\ddot{R}\hat{\rho}$, allowing us to find the following result for the TF density of a BEC in an expanding toroid:

$$n_0(\boldsymbol{r}) = \frac{1}{U}\Big(\mu(t) - \frac{1}{2}M\omega_z^2 z^2 - \lambda|\rho-R|^n - M\ddot{R}(\rho-R)\Big) \times\Theta\Big(\mu(t) - \frac{1}{2}M\omega_z^2 z^2 - \lambda|\rho-R|^n - M\ddot{R}(\rho-R)\Big), \tag{A5}$$

obtained by integrating both sides of Eq. (A4) with respect to ρ. Note we also plugged in $V(\boldsymbol{r},t)$ from Eq. (2), and an overall constant of integration was chosen so that the ρ dependence of Eq. (A5) is via the combination $\rho - R(t)$ (although we suppressed the time argument in R for brevity).

The chemical potential in Eq. (A5) is determined by satisfying the fixed number constraint $N = \int d^3r\, n_0(\boldsymbol{r})$, with N the total boson number. In this integration, the term proportional to $(\rho - R(t))$ will approximately vanish, with the other terms in Eq. (A5) determining the TF radii in the z and ρ directions, which are given by:

$$R_z = \sqrt{\frac{2\mu(t)}{M\omega_z^2}}, \tag{A6}$$

$$R_\rho = \Big(\frac{\mu(t)}{\lambda}\Big)^{1/n}. \tag{A7}$$

With these definitions, the density is given by:

$$n_0 \simeq \frac{\mu(t)}{U}\Big[1 - \frac{z^2}{R_z^2} - \frac{1}{R_\rho^n}|\rho-R|^n - \frac{M\ddot{R}}{\mu(t)}(\rho-R)\Big] \times\Theta\Big(1 - \frac{z^2}{R_z^2} - \frac{1}{R_\rho^n}|\rho-R|^n - \frac{M\ddot{R}}{\mu(t)}(\rho-R)\Big), \tag{A8}$$

describing a peak in the atom density that approximately follows the expanding ring. The large value of the exponent n implies a "flatness" to the density profile in the radial direction, i.e., a weak dependence of the density on ρ. We note that in the Eckel et al experiments the exponent $n \simeq 4$, although we'll keep it general in this section.

The system chemical potential $\mu(t)$ is determined by the requirement of a fixed total particle number N during expansion. Since the density at the center of the toroid (i.e. at $\rho = R(t)$ and $z = 0$) is proportional to $\mu(t)$ in Eq. (A8), and the toroid volume is proportional to $R_z R_\rho R(t)$, then the fixed number constraint leads to the estimate

$$N \propto \mu(t) R_z R_\rho R(t) \propto \mu(t)^{\frac{3n+2}{2n}} R(t), \tag{A9}$$

which implies the chemical potential satisfies

$$\mu(t) \propto R(t)^{-\frac{2n}{3n+2}}, \tag{A10}$$

with exponent $\gamma \equiv \frac{2n}{3n+2} \simeq \frac{4}{7}$. Thus, during expansion, the chemical potential (and central density) decrease with increasing time. Note that since the sound velocity $c \propto \sqrt{n_0}$, this result implies that the sound velocity scales with toroidal radius as $c \propto R(t)^{-\frac{1}{2}\gamma}$, or $R(t)^{-2/7}$ for the case of $n = 4$ [38].

We have found that a solution with $\boldsymbol{v} \simeq \dot{R}(t)\hat{\rho}$ can approximately satisfy the Euler equation and yields a time-dependent chemical potential in the number constraint equation. The next step is to examine the continuity equation, Eq. (A3), which is:

$$\partial_t n_0 = -\boldsymbol{\nabla} n_0 \cdot \boldsymbol{v} - n_0 \boldsymbol{\nabla} \cdot \boldsymbol{v}. \tag{A11}$$

We now analyze Eq. (A11) without assuming $\boldsymbol{v} \simeq \dot{R}(t)\hat{\rho}$, but only the TF density profile result Eq. (A5). To simplify the left side of Eq. (A11), we note that Eq. (A5) implies that the partial time derivative of n_0 satisfies:

$$\begin{aligned} \partial_t n_0 &= -\dot{R}(t)\hat{\rho} \cdot \boldsymbol{\nabla} n_0(\rho, z, t) \\ &+ \frac{1}{U}\Big(\partial_t \mu(t) - M(\rho - R(t))\ddot{R}(t)\Big). \end{aligned} \tag{A12}$$

Henceforth we drop the final term on the right side, since it is small in the regime $\rho \to R(t)$. Plugging this into the left side of Eq. (A11) gives

$$-\dot{R}(t)\hat{\rho} \cdot \boldsymbol{\nabla} n_0 + \frac{1}{U}\partial_t \mu(t) = -\boldsymbol{\nabla} n_0 \cdot \boldsymbol{v} - n_0 \boldsymbol{\nabla} \cdot \boldsymbol{v}. \tag{A13}$$

We now analyze this equation in the regime of $\rho \simeq R(t)$. From Eq. (A5), we find that the gradient of n_0 is a constant at $\rho \to R$ and is given by:

$$\hat{\rho} \cdot \boldsymbol{\nabla} n_0 \Big|_{\rho \to R(t)} = -\frac{M\ddot{R}(t)}{U}. \tag{A14}$$

Plugging this in to the continuity equation, using our result for μ (which implies $\partial_t \mu = -\gamma \frac{\dot{R}}{R}\mu$), and cancelling an overall factor of $1/U$, we find:

$$M\dot{R}\ddot{R} - \mu\gamma\frac{\dot{R}}{R} = M\ddot{R}v - \mu \boldsymbol{\nabla} \cdot \boldsymbol{v}. \tag{A15}$$

Now we take account of the fact that our system exhibits a rapid growth of R with increasing t. During this expansion, μ decreases slowly according to Eq. (A10), while $\frac{\dot{R}}{R}$ is $\mathcal{O}(1)$ (e.g. for exponential growth). This implies that the first terms on the right and left sides of Eq. (A15) are much larger than the second terms on the left and right sides. Dropping the subleading terms, we finally get:

$$M\dot{R}\ddot{R} = M\ddot{R}v, \tag{A16}$$

or $v = \dot{R}$, consistent with our original assumption. This shows that, within the preceding approximations, a rapidly expanding toroidal BEC indeed exhibits a radial superfluid velocity $\boldsymbol{v} = \dot{R}\hat{\rho}$.

[1] A. A. Starobinsky, *A New Type of Isotropic Cosmological Models Without Singularity*, Phys. Lett. B **91**, 99 (1980). doi:10.1016/0370-2693(80)90670-X

[2] A. H. Guth, *The Inflationary Universe: A Possible Solution to the Horizon and Flatness Problems*, Phys. Rev. D **23**, 347 (1981). doi:10.1103/PhysRevD.23.347

[3] A. Albrecht and P. J. Steinhardt, *Cosmology for Grand Unified Theories with Radiatively Induced Symmetry Breaking*, Phys. Rev. Lett. **48**, 1220 (1982). doi:10.1103/PhysRevLett.48.1220

[4] S. W. Hawking and I. G. Moss, *Supercooled Phase Transitions in the Very Early Universe*, Phys. Lett. **110B**, 35 (1982). doi:10.1016/0370-2693(82)90946-7

[5] A. D. Linde, *A New Inflationary Universe Scenario: A Possible Solution of the Horizon, Flatness, Homogeneity, Isotropy and Primordial Monopole Problems*, Phys. Lett. **108B**, 389 (1982). doi:10.1016/0370-2693(82)91219-9

[6] A. D. Linde, *Chaotic Inflation*, Phys. Lett. **129B**, 177 (1983). doi:10.1016/0370-2693(83)90837-7

[7] A. R. Liddle and D. H. Lyth, *Cosmological inflation and*

large scale structure, Cambridge, UK: Univ. Pr. (2000).

[8] A. Ijjas and P. J. Steinhardt, *Bouncing Cosmology made simple*, Class. Quant. Grav. **35**, no. 13, 135004 (2018). doi:10.1088/1361-6382/aac482

[9] P. A. R. Ade *et al.* [Planck Collaboration], *Planck 2015 results. XIII. Cosmological parameters*, Astron. Astrophys. **594**, A13 (2016). doi:10.1051/0004-6361/201525830

[10] M. Tegmark *et al.* [SDSS Collaboration], *Cosmological parameters from SDSS and WMAP*, Phys. Rev. D **69**, 103501 (2004). doi:10.1103/PhysRevD.69.103501

[11] J. E. Lidsey, A. R. Liddle, E. W. Kolb, E. J. Copeland, T. Barreiro and M. Abney, *Reconstructing the inflation potential : An overview*, Rev. Mod. Phys. **69**, 373 (1997). doi:10.1103/RevModPhys.69.373

[12] P. A. R. Ade *et al.* [Planck Collaboration], *Planck 2015 results. XX. Constraints on inflation*, Astron. Astrophys. **594**, A20 (2016). doi:10.1051/0004-6361/201525898

[13] P. A. R. Ade *et al.* [Planck Collaboration], *Planck 2015 results. XVI. Isotropy and statistics of the CMB*, Astron. Astrophys. **594**, A16 (2016). doi:10.1051/0004-6361/201526681

[14] C. Barcelo, S. Liberati and M. Visser, *Analogue gravity*, Living Rev. Rel. **14**, 3 (2011). doi:10.12942/lrr-2005-12

[15] W. G. Unruh, *Experimental black hole evaporation*, Phys. Rev. Lett. **46**, 1351 (1981). doi:10.1103/PhysRevLett.46.1351

[16] S. W. Hawking, *Black hole explosions*, Nature **248**, 30 (1974). doi:10.1038/248030a0

[17] S. W. Hawking, *Particle Creation by Black Holes*, Commun. Math. Phys. **43**, 199 (1975) Erratum: [Commun. Math. Phys. **46**, 206 (1976)]. doi:10.1007/BF02345020 doi:10.1007/BF01608497

[18] T. G. Philbin, C. Kuklewicz, S. Robertson, S. Hill, F. Konig and U. Leonhardt, *Fiber-optical analogue of the event horizon*, Science **319**, 1367 (2008). doi:10.1126/science.1153625

[19] F. Belgiorno *et al.*, *Hawking radiation from ultrashort laser pulse filaments*, Phys. Rev. Lett. **105**, 203901 (2010). doi:10.1103/PhysRevLett.105.203901

[20] S. Weinfurtner, E. W. Tedford, M. C. J. Penrice, W. G. Unruh and G. A. Lawrence, *Measurement of stimulated Hawking emission in an analogue system*, Phys. Rev. Lett. **106**, 021302 (2011). doi:10.1103/PhysRevLett.106.021302

[21] J. Steinhauer, *Observation of quantum Hawking radiation and its entanglement in an analogue black hole*, Nature Phys. **12**, 959 (2016). doi:10.1038/nphys3863

[22] T. Torres, S. Patrick, A. Coutant, M. Richartz, E. W. Tedford and S. Weinfurtner, *Rotational superradiant scattering in a vortex flow*, Nature Phys. **13**, 833 (2017). doi:10.1038/nphys4151

[23] J.-C. Jaskula, G. B. Partridge, M. Bonneau, R. Lopes, J. Ruaudel, D. Boiron and C. I. Westbrook, *Acoustic analog to the dynamical Casimir effect in a Bose-Einstein condensate*, Phys. Rev. Lett. **109**, 220401 (2012). doi:10.1103/PhysRevLett.109.220401

[24] C. L. Hung, V. Gurarie and C. Chin, *From Cosmology to Cold Atoms: Observation of Sakharov Oscillations in Quenched Atomic Superfluids*, Science **341**, 1213 (2013). doi:10.1126/science.1237557

[25] P. O. Fedichev and U. R. Fischer, *Gibbons-Hawking effect in the sonic de Sitter space-time of an expanding Bose-Einstein-condensed gas*, Phys. Rev. Lett. **91**, 240407 (2003). doi:10.1103/PhysRevLett.91.240407

[26] O. Fialko, B. Opanchuk, A. I. Sidorov, P. D. Drummond and J. Brand, *Fate of the false vacuum: towards realization with ultra-cold atoms*, EPL **110**, 56001 (2015). doi:10.1209/0295-5075/110/56001

[27] O. Fialko, B. Opanchuk, A. I. Sidorov, P. D. Drummond and J. Brand, *The universe on a table top: engineering quantum decay of a relativistic scalar field from a metastable vacuum*, J. Phys. B **50**, no. 2, 024003 (2017). doi:10.1088/1361-6455/50/2/024003

[28] J. Braden, M. C. Johnson, H. V. Peiris and S. Weinfurtner, *Towards the cold atom analog false vacuum*, JHEP **1807**, 014 (2018). doi:10.1007/JHEP07(2018)014

[29] T. P. Billam, R. Gregory, F. Michel and I. G. Moss, *Simulating seeded vacuum decay in a cold atom system*, Phys. Rev. D **100**, no. 6, 065016 (2019). doi:10.1103/PhysRevD.100.065016

[30] J. Rodriguez-Laguna, L. Tarruell, M. Lewenstein and A. Celi, *Synthetic Unruh effect in cold atoms*, Phys. Rev. A **95**, no. 1, 013627 (2017). doi:10.1103/PhysRevA.95.013627

[31] C. Barcelo, S. Liberati and M. Visser, *Probing semiclassical analog gravity in Bose-Einstein condensates with widely tunable interactions*, Phys. Rev. A **68**, 053613 (2003). doi:10.1103/PhysRevA.68.053613

[32] P. O. Fedichev and U. R. Fischer, *'Cosmological' quasiparticle production in harmonically trapped superfluid gases*, Phys. Rev. A **69**, 033602 (2004). doi:10.1103/PhysRevA.69.033602.

[33] U. R. Fischer and R. Schutzhold, *Quantum simulation of cosmic inflation in two-component Bose-Einstein condensates*, Phys. Rev. A **70**, 063615 (2004). doi:10.1103/PhysRevA.70.063615

[34] P. Jain, S. Weinfurtner, M. Visser and C. W. Gardiner, *Analog Model of a Friedmann-Robertson-Walker Universe in Bose-Einstein Condensates: Application of the Classical Field Method*, Phys. Rev. A **76**, 033616 (2007).

doi:10.1103/PhysRevA.76.033616

[35] A. Prain, S. Fagnocchi and S. Liberati, *Analogue Cosmological Particle Creation: Quantum Correlations in Expanding Bose Einstein Condensates*, Phys. Rev. D **82**, 105018 (2010). doi:10.1103/PhysRevD.82.105018

[36] J. M. Gomez Llorente and J. Plata, *Expanding ring-shaped Bose-Einstein condensates as analogs of cosmological models: Analytical characterization of the inflationary dynamics*, Phys. Rev. A **100**, no. 4, 043613 (2019). doi:10.1103/PhysRevA.100.043613

[37] Z. Fifer, T. Torres, S. Erne, A. Avgoustidis, R. J. A. Hill and S. Weinfurtner, *Analog cosmology with two-fluid systems in a strong gradient magnetic field*, Phys. Rev. E **99**, no. 3, 031101 (2019). doi:10.1103/PhysRevE.99.031101

[38] S. Eckel, A. Kumar, T. Jacobson, I. B. Spielman and G. K. Campbell, *A rapidly expanding Bose-Einstein condensate: an expanding universe in the lab*, Phys. Rev. X **8**, no. 2, 021021 (2018). doi:10.1103/PhysRevX.8.021021

[39] M. Wittemer, F. Hakelberg, P. Kiefer, J. P. Schröder, C. Fey, R. Schützhold, U. Warring and T. Schaetz, *Phonon Pair Creation by Inflating Quantum Fluctuations in an Ion Trap*, Phys. Rev. Lett. **123**, no. 18, 180502 (2019). doi:10.1103/PhysRevLett.123.180502

[40] M. Sasaki, *Gauge Invariant Scalar Perturbations in the New Inflationary Universe*, Prog. Theor. Phys. **70**, 394 (1983). doi:10.1143/PTP.70.394

[41] H. Kodama and M. Sasaki, *Cosmological Perturbation Theory*, Prog. Theor. Phys. Suppl. **78**, 1 (1984). doi:10.1143/PTPS.78.1

[42] V. F. Mukhanov, *Quantum Theory of Gauge Invariant Cosmological Perturbations*, Sov. Phys. JETP **67**, 1297 (1988) [Zh. Eksp. Teor. Fiz. **94N7**, 1 (1988)].

[43] P. J. E. Peebles, "Principles of physical cosmology," Princeton, USA: Univ. Pr. (1993).

[44] S. Weinberg, "Cosmology," Oxford, UK: Oxford Univ. Pr. (2008).

[45] N. D. Birrell and P. C. W. Davies, *Quantum Fields in Curved Space*, Cambridge Univ. Pr. (1984).

[46] V. Mukhanov and S. Winitzki, *Introduction to quantum effects in gravity*, Cambridge Univ. Pr. (2007).

[47] L. Parker and D. Toms, *Quantum Field Theory in Curved Spacetime: Quantized Fields and Gravity*, Cambridge Univ. Pr. (2009).

[48] S. M. Carroll, "Spacetime and Geometry," San Francisco, USA: Addison-Wesley (2004).

[49] I. Carusotto, S. Fagnocchi, A. Recati, R. Balbinot and A. Fabbri, *Numerical observation of Hawking radiation from acoustic black holes in atomic BECs*, New J. Phys. **10**, 103001 (2008). doi:10.1088/1367-2630/10/10/103001

[50] M. Naraschewski and R. J. Glauber, *Spatial coherence and density correlations of trapped Bose gases*, Phys. Rev. A **59**, 4595 (1999). doi:10.1103/PhysRevA.59.4595

[51] M. Schellekens, R. Hoppeler, A. Perrin, J. Viana Gomes, D. Boiron, A. Aspect, C. I. Westbrook, *Hanbury Brown Twiss Effect for Ultracold Quantum Gases*, Science **310**, 648 (2005). doi:10.1126/science.1118024

[52] V.I. Yukalov, *Theory of cold atoms: Bose-Einstein statistics*, Laser Physics **26**, 062001 (2016). doi:10.1088/1054-660X/26/6/062001

[53] G. Baym and C.J. Pethick, *Ground-State Properties of Magnetically Trapped Bose-Condensed Rubidium Gas*, Phys. Rev. Lett. **76**, 6 (1996). doi:10.1103/PhysRevLett.76.6

[54] A. Imambekov, I. E. Mazets, D. S. Petrov, V. Gritsev, S. Manz, S. Hofferberth, T. Schumm, E. Demler, and J. Schmiedmayer, *Density ripples in expanding low-dimensional gases as a probe of correlations*, Phys. Rev. A **80**, 033604 (2009). doi:10.1103/PhysRevA.80.033604